ISSN 2347-3487

Investigation of Structural, Magneto-transport, and Electronic properties of $Pr_{0.7}Sr_{0.3}MnO_3$ nanoparticle

Proloy T. Das, and T. K. Nath

Department of Physics, Indian Institute of Technology Kharagpur,
Kharagpur - 721302, India.
dasproloy@phy.iitkgp.ernet; tnath@phy.iitkgp.ernet.in

ABSTRACT

In this report Micro-structural, magnetic, electronic, and magneto-transport properties of perovskite $Pr_{0.7}Sr_{0.3}MnO_3$ manganite nanoparticles have been thoroughly investigated. A series of samples with different particle size (Φ) is synthesized by chemical 'pyrophoric' reaction process. Rietveld refinement of X-Ray diffraction pattern of the sample showed single phase orthorhombic structure with Pbnm space group. Metal - insulator transition (T_P) has been observed in the temperature range of 180-200 K in zero field resistivity data (2 – 300 K) and it differs from ferromagnetic to paramagnetic transition temperature (T_C) due to enhanced surface disorder effect. The lowest nanomentric sample exhibit maximum 85 % magneto-resistances under 8 T magnetic field at 4 K. Magneto-impedance measurement of the $Pr_{0.7}Sr_{0.3}MnO_3$ nano particles have been obtained at 0.8 T in the temperature range 80-300 K. The magneto transport properties has been explored with spin polarized tunneling and spin dependent scattering of single ferromagnetic domain with nanometric grain size modulation. We have analyzed temperature dependent resistivity data using small polaron hopping and variable range hopping models. Below < 40 K a resistivity upturn behavior exhibiting a distinct resistivity minimum has been observed for each sample, which is best explained by electron-electron interaction and weak localization mechanism.

Indexing terms/Keywords

Manganite nanoparticles; Microstructure; Magnetoresistance; Spin polaron hopping; Variable range hopping

Pacs

72.25.Dc, 73.63. Bd, 75.47.Lx, 75.75.Fk,

ISSN 2347-3487

1.0 INTRODUCTION

The perovskite manganites with generic formula $Re_{1-x}R_xMnO_3$, where Re is trivalent rare earth cation (e.g. La, Pr, Nd etc.) and R is divalent alkaline earth cation (e.g. Ca, Sr, Ba, Pb etc.) have drawn considerable attention, especially following the discovery of their colossal magneto-resistive (CMR) [1-5] property. In these materials subtle balance between charge, spin, lattice and orbital degrees of freedom leads to a variety of phases with fascinating properties like charge ordering (CO) and orbital ordering (OO) [6-8], insulator-metal (MIT) transition [3, 9], ferromagnetic insulator (FMI) phase, canted anti-ferromagnetic insulator [10, 11] phase and so on. Magneto-resistive (MR) property in manganites is believed due to the Zener double exchange (DE) [12] mechanism mediated by hopping of e_g electron from Mn^{3+} to Mn^{4+} ion, which helps to drive into the ferromagnetic metallic (FMM) phase. In the bulk polycrystalline or single crystal sample, DE mechanism strongly correlates with electronic, magnetic, and magnto-transport properties.

However, in nanometric dimension due to enhanced surface effect having high surface to volume ratio this correlation is not preserved and as a result a different kind of transport and magnetic properties come into picture. In nanometric grain size modulation, change in electronic-, magneto-transport, and other physical properties appears due to mainly finite size effect. The doping with alkaline earth cations (Sr, Ca, Ba) doped in rare earth Pr site in $PrMnO_3$ manganites show interesting properties because of the large difference between the Pr and Sr, Ca, Ba ionic radii. A number of reports have already have been published [13-19] focusing on different physical properties of Pr- based manganite, although there is no detail systematic study on $Pr_{0.7}Sr_{0.3}MnO_3$ (PSMO) in nanometric scale.

In the present work, we have investigated in detail nano size induced grain boundary effect on hole doped $Pr_{0.7}Sr_{0.3}MnO_3$ compound in terms of electronic and magnetic transport properties under large external magnetic fields (H_{ext}).

2.0 EXPERIMENTAL DETAILS

A series of nanometric PSMO samples were synthesized through chemical pyrophoric reaction process by making solution of Pr_6O_{11}, $Sr(NO_3)_2$ and Mn $(CH_3COO)_2$ in required stoichiometric ratios. Then triethanolamine (TEA) is added with the starting solutions maintaining metal ions to TEA ratio at 1:1:5 (Pr, Sr: Mn: TEA=1:1:5) to make a viscous solution. The mixed solutions are kept on a hot plate at 200^0C with continuous stirring. After foaming and puffing of this solution, a black fluffy powder is obtained [20] through gel combustion process and it is calcined at various temperatures (850, 950, and 1050^0C for 5 hours) to get a series of PSMO nanocrystalline powders. Therefore, the sintering effect can only be to glue one grain to the other.The sintered powders were pressed to make a circular pellet at a pressure of 6 Tons and cut in a bar like structure and then sintered for two hours at corresponding calcinations temperature after amalgamations of grain. Structural characterization of PSMO samples were characterized by X-ray diffraction pattern (Philips PW1710 model) with Cu-K_α radiation (λ ~1.542 Å) to investigate proper phase of the sample. Selected area diffraction pattern (SAED) and Transmission electron microscopy (TEM) image of the samples were recorded using JEOL 2010F UHR version electron microscope at an accelerating voltage of 200 kV to investigate the particle size and micro-structure of the samples. DC- magnetization and temperature dependence complex ac-susceptibility ($\chi = \chi' + \chi''$) of each PSMO sample was measured by homemade vibrating sample magnetometer (VSM) and ac-susceptibility set up [21], with a lock-in-amplifier (Stanford Research SR 830), a temperature controller (Lakeshore S331), a variable temperature cryostat (JENIS). Low field magneto-impedance (LFMI) measurement is also carried out in the temperature range of 77-300 K using a solenoid coil magnet of 1T, employing a HIOKI 3532-50 LCR Hi-TESTER meter. During LFMI measurement we have fixed the dc current at a certain value and tuned the frequency range from 100 kHz to 2 MHz. Temperature dependence of dc- resistivity and magneto-resistance (MR) of PSMO samples were measured down to 4 K by a standard four probe contact method using a high field low temperature set up (8 T CFM VTI, CRYOGENIC Ltd., U.K.). Low-field MR (LFMR) down to 77 K at H_{ext} of 0.5 T was carried out by constant flow liquid nitrogen set up.

3.0 RESULTS AND DISCUSSIONS

3.1 Structural properties

The orthorhombic crystal structure with Pbnm space group of this PSMO system has been found after Rietveld refinement of XRD pattern recorded at room temperature as shown in Fig. 1(a). Crystallite size of the samples has been calculated using Debye-Scherrer formula, ($\varphi = k\lambda / \beta_{eff} \cos\theta$) for the most intense peak, where Φ, λ, β_{eff}, θ denotes crystallite size, Cu K_α wavelength (1.542 Å), full width at half maximum (FWHM) of the peak, and scattering angle respectively. In the present work, we have considered shape factor, k' as 0.9. The average crystallite sizes of the samples are obtained as 28nm, 37nm, and 42 nm when sintered at 850^0C, 950^0C, 1050^0C respectively and it varies linearly with sintering temperatures. In the Figs. 1(b-d), we have shown micro structural properties like high resolution TEM, and SAED pattern respectively.

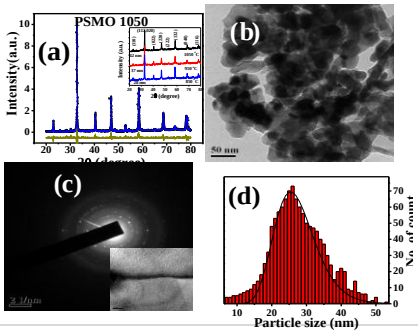

Figure 1. (color online) (a), and inset (a) Rietveld refinement of HRXRD of PSMO 1050 sample and normal XRD of all PSMO samples; (b) High resolution TEM image, (c) and inset of (c) SAED pattern and lattice fringe of PSMO 850 sample, (d) Histogram of PSMO 850 sample.

ISSN 2347-3487

Bright field TEM micrographs depict that the particles are in nanometric regime and the estimated interplaner lattice spacing d ~ 3.501 ± 0.001 Å from high resolution TEM lattice fringes data corroborate with (111) plane of the crystal. SAED pattern from a single grain confirms the polycrystalline nature of the sample. Particle size distribution of our polydispersive PSMO 850 sample is shown in Fig. 1(c) and obtained average particle size as 28 nm which is less than the critical limit (70 nm) [22]. Extracted micro-structural parameters using Rietveld refinement of XRD pattern are listed in Table 1. Any finite change in volume and r. m. s. microstarin values of these nanometric samples are not observed in the present case.

Table 1. Different physical parameters estimated from Rietveld refinement (lattice parameters, unit cell volume, micro-strains).

Sample PSMO	a (Å)	b (Å)	c (Å)	Unit cell volume ($Å^3$)	r. m. s micro-strain	χ^2
850	5.479	5.464	7.711	163.564	0.0012	0.0577
950	5.479	5.457	7.713	163.173	0.0008	0.0687
1050	5.465	5.487	7.735	164.561	0.0013	0.0383

3.2 Magnetic Properties

Magnetic hysteresis loop as a function of magnetic field for PSMO samples are shown in Fig. 2.

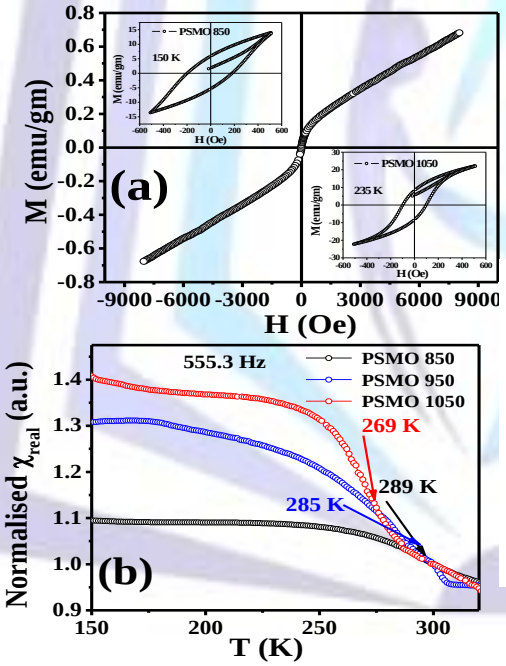

Figure 2. (color online) Magnetic hysterias as a function of magnetic fields: (a) PSMO 950 sample at 300 K, inset of (a) [left upper panel] and [right lower upper panel]: ferromagnetic hysteresis of PSMO 850 sample at 150 K, and of PSMO 1050 sample at 235 K respectively, and (b) Complex linear ac-susceptibility behavior with temperature of PSMO samples. Arrow indicates T_C of the corresponding sample.

No saturation magnetization has been observed within the measured magnetic field scale; however all the samples exhibit good ferromagnetic hysteresis loop with spontaneous magnetization confirming ferromagnetic metallic ground state of PSMO system. Figure 2(b) depicts the temperature dependent complex ac-susceptibility measurement of all the samples.

The derivative of the AC-susceptibility data ($d\chi'/dT$) provides the ferromagnetic to paramagnetic transition temperature (T_C). It has been observed that, for nanometric samples T_C varies between 278 - 287 K and it increases by ~ 30 K compare to reported conventional bulk system (~250 K) [23, 24]. Observed relative widening of ferromagnetic to paramagnetic transition region could most likely due to distribution of the exchange interaction strength which is developed at the nonmagnetic surface of the grain in this kind of correlated system. This kind enhancement of T_C mainly due to enhanced DE interaction in the nanoparticles as reported by Sarkar et al. [25].

3.3 Magneto Transport

The CMR property in single crystal manganites is mainly due to enhancement of transfer integral t_{ij} via suppression of spin fluctuation (MR_{INT}) by the applied magnetic field. In polycrystalline sample, another important contribution of MR appears due to field dependent spin polarized tunneling (MR_{SPT}) part. In order to find out field

dependent contributions of MR_{SPT} and intrinsic magneto resistance (MR_{INT}) approximately in total observed MR in the present PSMO system, we have considered the scheme neglecting magnetic scattering at domain boundary [26] as used by Raychaudhuri et al. [27] and can be expressed as,

$$MR = -A\int_0^H f(k)dk - JH - KH^3 \quad \text{.....(1)}$$

where, '*k*' is the pinning strength. The grain boundary have a distribution of pinning strengths (defined as the minimum field needed to overcome a particular pinning barrier) given by f(k) expressed as,

$$f(k) = A\exp(-Bk^2) + Ck^2\exp(-Dk^2) \quad \text{.....(2)}$$

The field dependent MR_{INT} term with the adjustable parameters a, b, and the spin polarization part (MR_{SPT}) with adjustable fitting parameters A, B, C, D, J and H can be defined as,

$$MR_{INT}(H) = -aH - bH^3; MR_{SPT} = -\int_0^H f(k)dk \quad \text{.....(3)}$$

Using Eqn. (3) we have calculated low field MR contributions (MR_{SPT} and MR_{INT}) from the extracted fitting parameters within the approximation of the model and it has been summarized in Table – 2.

Table 2. Various LFMR components of PSMO samples at 77 K; Field dependence of residual resistivity, activation energies (W) and Density of states at E_F of PSMO samples with error bar.

Sample PSMO	MR_{SPT}	MR_{INT}	MR_{EXP}	MR	H_{EXT} (T)	ρ_0 ($\times 10^{-4}$ Ω-cm K^{-1})	Activation energy (W) (meV)	$N(E_F)$ ($\times 10^{19}$ $eV^{-1}cm^{-3}$)
850	-8.54	-11.54	-20.08	-20.3	0	a)1.123 (<250 K) b)1.031 (280 to 320K)	a)117.08 b)150.47	18.2 (±0.001)
					1	a)1.058 (<260 K) b)1.022 (280 to 320K)	a) 124.03 b)147.31	17.2 (±0.002)
					8	a)1.085 (<270 K) b)1.011 (280 to 320K)	a)91.71 b)142.96	17.8 (±0.002)
950	-6.95	-12.21	-19.16	-19.4	0	a)1.116 (<260 K) b)1.090 (280 to 320K)	a) 106.12 b) 111.64	6.59 (±0.001)
					1	a)1.124 (<260 K) b)1.038 (280 to 320K)	a)102.73 b)134.28	11.9 (±0.002)
					8	a)1.285 (<260 K) b)1.087 (280 - 320K)	a) 77.15 b) 103.49	51.2 (±0.002)
1050	-21.63	-2.63	-15.85	-16.1	0	a)1.012 (<260 K) b)1.00 (280 to 320K)	a)119.82 b)197.55	5.41
					1	a)1.012 (<260 K) b)1.00 (280 to 320K)	a) 116.81 b)183.36	7.85
					8	a)1.084 (<260 K) b)1.007 (280 to 320K)	a) 60.68 b)123.40	103.2

From the Table 2, it is evident that MR_{SPT} part increases with particle size (~1.53%) compare to lowest nanometric size, whereas MR_{INT} part decreases (~2.38%) in highest nanometric size compared to other nanometric samples. The expected

ISSN 2347-3487

MR and calculated MR using Eq. (1) matches well for each sample. It is expected that field dependent MR is related to the spin polarized inter grain tunneling and spin dependant scattering across the grain surfaces which causes field induced - suppression of local magnetic disorder near grain boundary. In polycrystalline sample, CMR is related to the intrinsic properties of a system which occurs around T_C. Here, Figs. 3 (a-d) exhibit field dependence of MR at different temperatures for all PSMO samples. We have observed maximum 85% change in MR near T_P (~157 K) of PSMO 850 sample which corroborates with CMR property of the present system. For other two PSMO nano metric samples, we have observed maximum 83.5% (at 150 K for PSMO 950) and 82.3% (at 150 K for PSMO 1050) change in MR as shown in Fig. 3(b-c) respectively. In the inset of Fig. 3(b) low field magneto resistance (LFMR) variation of PSMO 950 is plotted for various temperatures. A combined comparative MR behavior of all samples at 150 K has shown in Fig. 3 (d), however all the samples show same value of MR (~80 %).

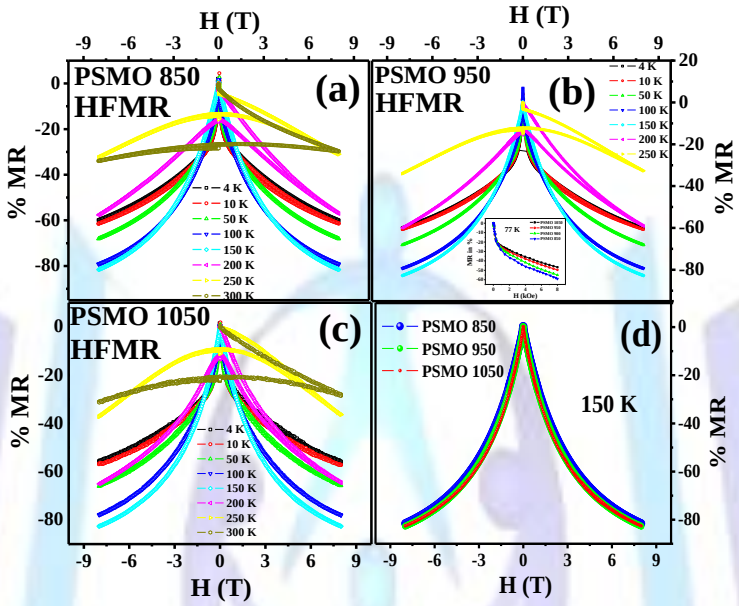

Figure 3. (color online) (a - c) HFMR of PSMO samples at different temperature; inset of (b), depicts LFMR of PSMO 950 sample at various temperatures; (d) Combined HFMR behavior of all samples at 150 K.

A strong temperature dependence (down to 77 K) and frequency (up to 2 MHz) of low field complex magneto impedance (LFMI) [= {Z(ω,H,T) – Z(ω, 0, T)}/ Z(ω, 0, T)] has been observed for all PSMO samples [15] as shown in Fig. 4.

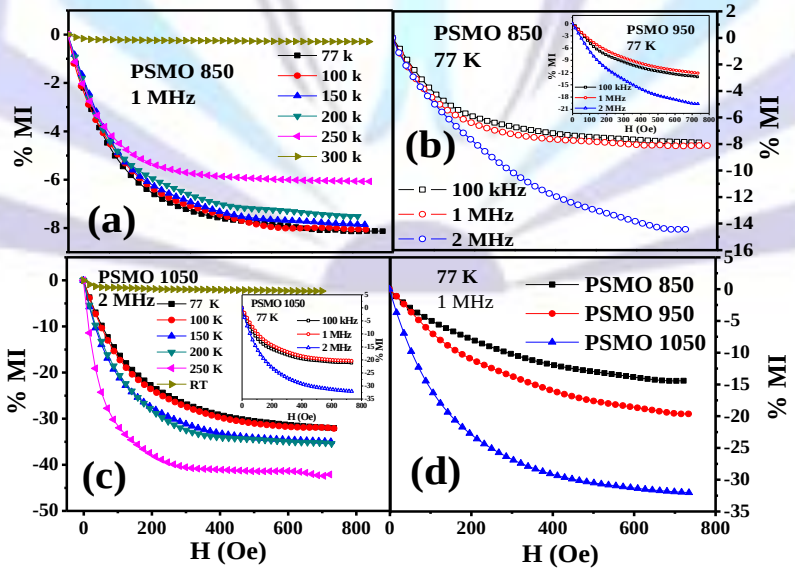

Figure 4. (color online) LFMI behavior of:(a) PSMO 850 sample at 1 MHz and at different temperatures; (b) PSMO 850, and 950 samples at 77 K and at different frequencies; (c) PSMO 1050 at 2 MHz and at different temperatures; inset of (c) PSMO 1050 sample at various frequencies at 77 K, and (d) all PSMO samples at 77 K and 1 MHz frequency.

It has been found that maximum 45 % change in MI at 250 K of PSMO 1050 sample compared to lowest nanometric samples, PSMO 850. Figure 4(d) depicts combined MI plot of all of PSMO samples as a function of magnetic field at 77 K

ISSN 2347-3487

and at a frequency of 1 MHz. The maximum percentage change in MI has been found -21% at 2 MHz by sweeping the dc magnetic field upto 800 Oe is found in PSMO 950 sample whereas PSMO850 sample exhibit maximum -8% change in MI at lowest attainable temperature (77 K) and at 1 MHz almost there is no change at room temperature. In higher frequency range, most likely the skin penetration depth becomes smaller and charge carrier conduction process along the surface region of the PSMO samples increases due to the skin depth effect (δ) of electrodynamics producing a moderate value of MI [16]. It has been found that, beyond 2 MHz range, coil ferromagnetic resonance [28-30] dominates over sample MI value, thus it is neglected.

3.4 Electronic Properties

Electronic dc-resistivity, ρ (T, H) of the polycrystalline PSMO compound down to 4 K has been measured using standard four probe dc-techniques as shown in Fig. 5 (a-c).

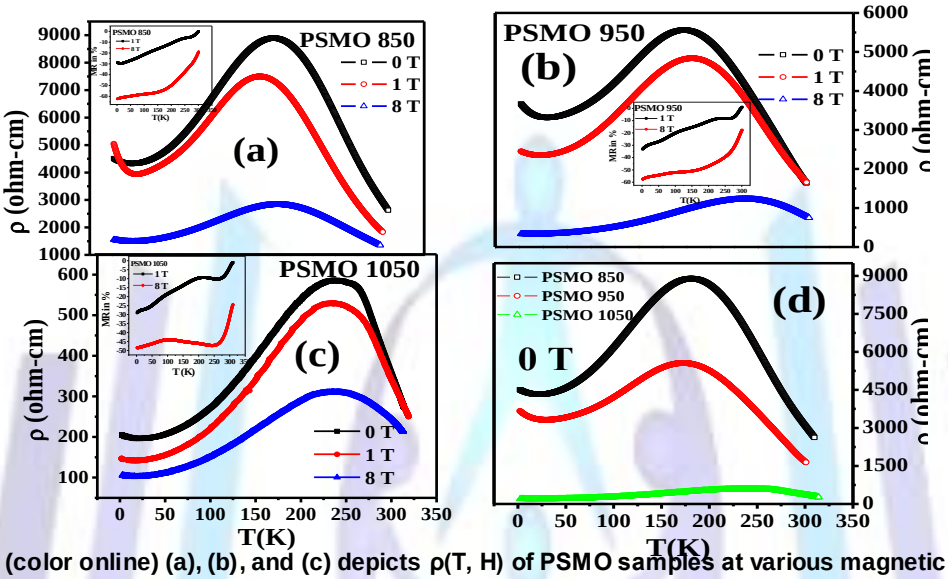

Figure 5. (color online) (a), (b), and (c) depicts ρ(T, H) of PSMO samples at various magnetic fields; Inset of (a), (b), and (c) shows corresponding MR% change with temperature of each sample, and (d) combined ρ(T) plot at zero field.

It has been found that peak resistivity value of PSMO 850 decreases (~13.91%) compared to PSMO 1050 at 0 T. Each sample exhibits a distinct metal-insulator (MIT) transition below which metallic conductive behavior appears whereas above MIT, it shows a semiconductor-like conductive behavior. This MIT transition temperature is suppressed with applied of magnetic fields due to reduction of surface disorder at the grains.

We have already discussed earlier that maximum MR of each PSMO nanometric samples have been found near their corresponding MIT temperature which reveals the existence of CMR property in ferromagnetic PSMO nanoparticles. In Fig. 5 (d), a combined ρ(T) picture of all PSMO samples at zero magnetic field is presented where modulation of MIT behavior with grain size is revealed. Porosity effect in this nanometric manganite has not been found a significant role on MIT, is reported elsewhere [20]. We believe that, for nano-crystalline sample due to enhanced surface to volume ratio, the breaking of Mn-O-Mn bond and scattering of charge carrier at the grain surfaces are modifying transport mechanism of present PSMO compound. More interestingly, MIT temperature of PSMO samples have been shifted toward lower temperature regime with reduction of grain size however no shift of T_C has been observed. Mainly decreasing of blocking temperature ($<<T_C$) (where electrons can conduct through more ordered core moments using small polaron tunneling mechanism) in this type of disordered manganite causes drop in MIT temperature [20] and breaking of Mn-O-Mn bond, scattering of charge carrier at the grain surfaces could also hinder inter-grain transport mechanism. This affects on resistivity value as shown in Fig. 5 (d).

We have investigated electronic transport mechanism of PSMO compound in depth and thoroughly analyzed the observed experimental ρ (T,H) data using various plausible models. Firstly, we have introduced small polaron hopping (SPH) model, which can be expressed as (non adiabatic approximation approach) [31, 32]

$$\rho = \rho_0 T \exp\left(\frac{W}{k_B T}\right) \quad \text{.....(4)}$$

where T, W and ρ_0 corresponds absolute temperature, activation energy and pre-exponential factor, $[k_B / \upsilon_{ph} Ne^2R^2C(1-C)]\exp(2\alpha R)$. Here k_B is Boltzmann constant, υ_{ph} is the optical phonon frequency, N is number of transition metal ions per unit volume, R is the average hopping distance, C is the fractional occupancy of the polarons, and α is the tunneling probability of electronic wave functional decay constant respectively. We have found that Eq. (4) fits well with ρ (T) data of all PSMO samples and calculated polaronic radius (r_p) which has the form of $(1/2)[\pi / 6N]^{1/3}$, lies within few angstrom

order (< 1.50 Å) for present PSMO sample justify the applicability of SPH model in paramagnetic regime through polaronic hopping conduction process. These small polarons occupy a fractional portion of unit cell volume and localized in that area as well. Pre-exponential factor (ρ_0), can be extracted using ln(ρ/T) vs T^{-1} plot shown in Figs. 6 (a-b) for PSMO 850, 950 samples respectively which is also tabulated (including PSMO 1050) in Table 2.

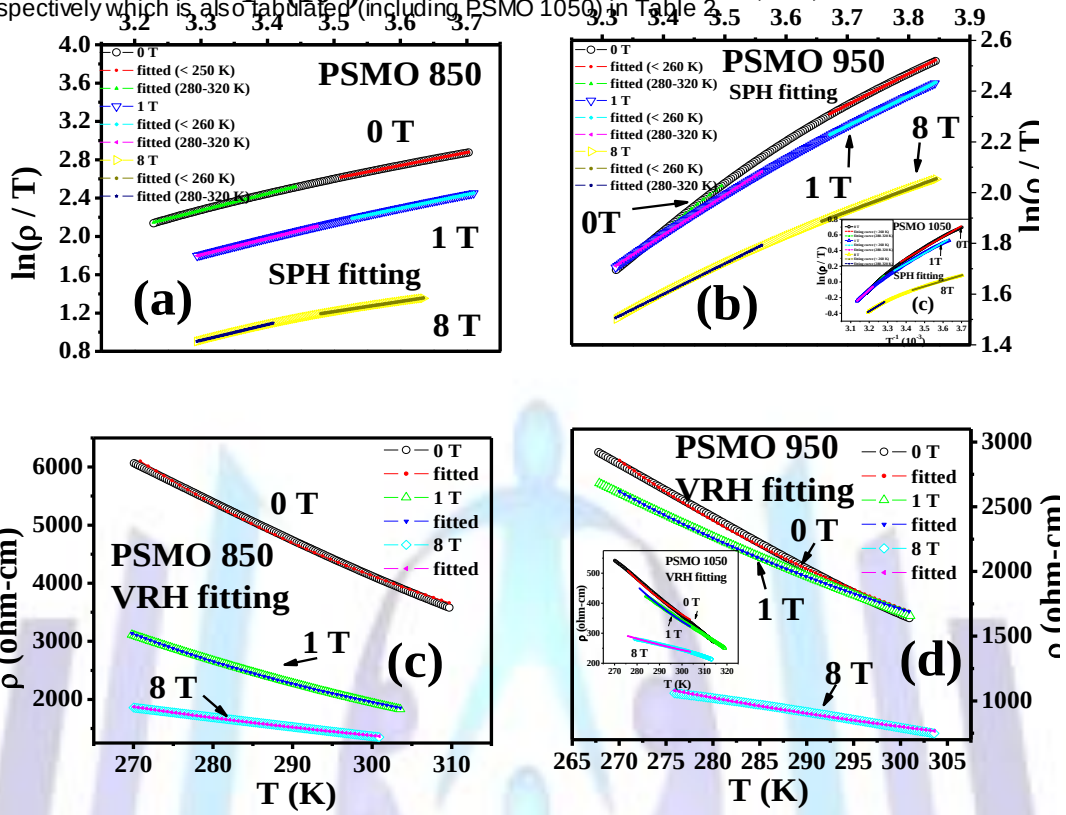

Figure 6. (color online) (a)-(b) Excellent SPH fitting of PSMO samples with various slopes in different temperature regime at 0, 1, and 8 T; (c)-(d) VRH fitting of PSMO samples at 0, 1, and 8 T respectively.

Due to presence of various slopes in different temperature regime curve could not be fit using Eq. (4) within whole range. Because of that we split it into different temperature ranges and fit with the Eq. (4). Fitted result gives a higher value of ρ_0 at low temperature regime due to mainly localization of electrons. Higher values of α at low temperature regime signify enhanced magnetic disorder whereas other parameters remain almost constant. Activation energy (W) cannot be responsible for the higher value of resistivity at low temperature because of its decreasing tendency at lower temperature regime. We have also investigated the magnetic field dependence of W which shows decreasing nature of W (0.28%, 0.37%, and 0.97% for PSMO 850, 950, 1050 samples respectively) at 8 T (in < 250 /260/270 K regime) which confirms delocalization and highly aligning nature of spins have been summarized in Table 2. Interestingly, in our case W is higher for PSMO 850 sample compare to other two samples; similar kind nature of W is already reported for NSMO nanomanganite [32]. We are also interested to see the effect of H_{EXT} on W in nanometric grain size modulation and the results are tabulated in Table 2.

In paramagnetic regime, we have fit ρ (T, H) data of all samples considering to Mott's variable-range hopping (VRH) model [33] which has the form,

$$\ln\left[\frac{\rho}{\rho_\infty}\right] = \left[\frac{T_0}{T}\right]^{\frac{1}{4}} \quad \text{.....(5)}$$

This VRH model was originated to explain the electronic conduction process of doped semiconductors where electrons acquires a hydrogenic orbitals of wave function $\psi=\psi_0 \exp(-\alpha r)$ and is localized by the potential fluctuation of dopant. The hopping mechanism of electrons could be conducted due to competitive nature of potential fluctuation and the onsite distance (R) of electrons. The hopping rate at a particular site R and at a given energy value ΔE can be calculated using,

$$\gamma = \gamma_0 e^{\left[-2\alpha r - \Delta E / k_B T\right]} \quad \text{.....(6)}$$

This hopping rate could be minimized using the lowest value of ΔE [$= \frac{4}{3}\pi R^3 N(E)]^{-1}$ and $R\{=(9/[8\pi\alpha\, N(E)\, k_B T])^{1/4}\}$ and express the modifies Mott resistivity as,

$$\rho = \rho_\infty \; e^{2.06\left[\frac{\alpha^3}{N(E)k_B T}\right]^{1/4}} \quad \text{.....(7)}$$

ISSN 2347-3487

which is reported by Viret et al.[34]. We have also calculated the density of available states of charge carriers at E_F (α =2.22 nm^{-1} assumed) employing the equation,

$$k_B T_0 = \frac{18\alpha^3}{N(E)} \quad \text{.....(8)}$$

and it is summarized in Table 2. We have found in this case, calculated N(E) values (~ 10^{19} $eV^{-1}cm^{-3}$) is quiet reasonable compare to other manganite systems[35]. Experimental data fits well with VRH model (R^2~ 99.999 for all PSMO samples) than SPH model in paramagnetic regime is shown in lower panel of Fig. 6.

In low temperature regime (< 40 K) below MIT, a distinct resistive anomaly has been observed in the present PSMO ferromagnetic metallic compound. This uptum of resistivity at low temperature regime in correlated manganite system attributed to the highly spin disorder, electron scattering inhomogeneous magnetic matrix of the system [36]. Observation and analyze of this resistive anomaly is an interesting issue over decades. The possible conduction mechanism in the ferromagnetic metallic regime below M-SC transition can be expressed as,

$$\rho(T) = \rho_0 - \rho_{e'} T^{\frac{1}{2}} + \rho_n T^n \quad \text{.....(9)}$$

Where ρ_0 the residual resistivity, contributed by elastic scattering likes electron – impurity scattering and coulomb interaction, $T^{1/2}$ term comes due to electron-electron interference effects (in presence of weak localization) [37, 38] T^n contribution comes from inelastic scattering effect (combined of electron-magnon, inelastic electron-electron and electron-phonon interactions [28]. ρ_e is coefficient for electron-electron-electron interference effect ~ $D^{-1/2}$ (diffusion constant), and n is inelastic scattering exponent for possible inelastic interaction. We have also tried to fit this resistive anomaly with various existing models like Kondo like mechanism, Coulomb blockade interaction etc. however the best fitted of experimental data for PSMO 850, and PSMO 950 nanometric samples has been found employing Eq. (9) which are shown in Figs. 7 (a), 7(b) respectively.

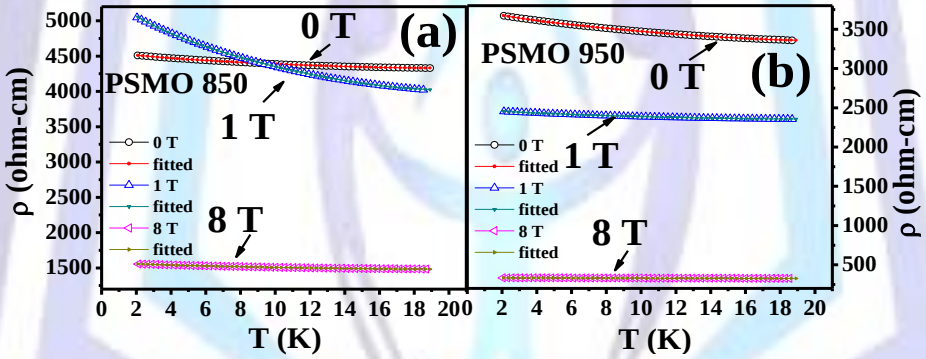

Figure 7. (color online) (a-b) depicts best fitted graphs of low temperature resistivity data employing Eq. 9 for PSMO 850, 950 samples.

We believe that the uptum of resistivity at low temperatures for PSMO 850, 950, and 1050 samples attributed the signature of highly spin disorder, increases of impurity, CI, scattering of electrons in magnetic inhomogeneity.

4. CONCLUSIONS

In summary, we have investigated in details the structural, magnetic-, magneto-transport, and electronic transport properties of $Pr_{0.7}Sr_{0.3}MnO_3$ compound in nanometric grain size modulation. More interestingly, we have found enhancement of T_C (~30 K) in PSMO nanometric samples compare to the T_C of bulk counterpart. A moderate MI values at higher frequency range has been observed in this compound which indicates the surface conduction mechanism enhances and penetration depth decreases gradually in this kind of nanomanganites due to higher value of surface to volume ratio in nanometric scale. The electronic- and magneto- transport properties of PSMO are found to have a strong dependence on nanometric particle size (φ). We have also analyzed the domain contribution in MR and it has been found that due to MR_{SPT} contribution of conduction e_g electrons between adjacent ferromagnetic grains enhances with the decrease of PSMO particle size. The nano size induced grain boundary effect is believed to be responsible for this modification of MIT temperature. Observed steeper slope of the upturn of resistivity in low temperature regime (<$T\rho_{min}$) of PSMO 850 sample compare to PSMO 1050, could be correlated with charging energy (E_C) or electron-electron interaction mechanism. Decreasing nature of MIT transition temperature with size reduction of the PSMO samples is explained well by SPT mechanism between two adjacent grains. The observed upturn of resistivity for all the samples < 40 K is explained by electron-electron interaction mechanism. We believe that in the PSMO system, it is possible to achieve a desired moderate MR value (far from optimal value) by controlling the temperature and could be used for technological application in various magnetic storage devices.

5. ACKNOWLEDGEMENTS

This research is supported by different funding agencies: (a) DAE (BRNS) through project S.L. No. 2006/37/52/BRNS/2376, dated 16.01.2007 (b) DST through project no. IR/S2/PU-04/2006 and (c) CSIR through Award no.: 09/081 (1077)/ 2010-EMR-I.

6. REFERENCES

[1] R. von Helmolt, J. Wecker, B. Holzapfel, L. Schultz, K. Samwer, Phys. Rev. Lett., 71, 1993, p. 2331.

[2] K. Chahara, T. Ohno, M. Kasai, Y. Kozono, Appl. Phys. Lett., 63,1993, p.1990.

[3] Colossal magneto resistive oxides by Y. Tokura, Gordon and Breach Science Publishers;

C. N. R. Rao, B. Raveau, Colossal Magnetoresistance, Charge Ordering and Related Properties of Manganese Oxides, World Scientific, Singapore,1998.

[4] S. Jin, T. H. Tiefel, M. McCormack, R. A. Fastnatch, R. Ramesh, L.H. Chen, Science, 264, 1994, p.413.

[5] H. L. Ju, C. Kwon, Q. Li, R. L. Greene, T. Venkatesan, Appl. Phys. Lett., 65, 1994, p.2108.

[6] Y. Tomioka, A. Asamitsu, Y. Moritomo, H. Kowakawa and Y. Tokura, Phys. Rev. Lett.,74, 1995; p.5108.

[7] H. Kuwahara, Y. Tomioka, A. Asamitsu, Y. Moritomo, and Y. Tokura, Science, 270,1995, p.961.

[8] V. Taphuoc, R. Sopracase, G. Gruener, J. C. Soret, F. Gervais, A. Maignan, C. Martin, Mat. Sci. and Eng. B,104, 2003, p.131.

[9] M. Imada, A. Fujimori, Y. Tokura, Rev. of Mod. Phys.,70, 1998, p.1216.

[10] E. Dagotto, T. Hotta, A. Moreo, Phys. Rep., 344, 2001, p.153.

[11] E. L. Nagaev, Phys. Rep., 346, 2001, p.387.

[12] C. Zener, Phys. Rev., 82, 1951, p.403.

[13] D. Dimitrov, V. Lovchinov, M. Gospodinov, and S. Dobreva, J. Mat.Sc.: Materials in Electronics, 14, 2003, p.765.

[14] X. C. Martin, A. Maignan, M. Hervieu, and B. Raveau, Phys. Rev. B, 60, 1999, p.12191.

[15] C. Lu, T. Z. Sholklapper, C. P. Jacobson, S. J. Viso, L. C. De Jonghe, J. Electrochem. Soc., 153, 2006, p.A1115.

[16] R. D. Shannon, Acta Cryst. A, 32, 1976, p.751.

[17] V. Sen, N. Panwar, G. L. Bhalla, S. K. Agarwal, J. All. Comp., 439, 2007, p.205.

[18] W. Boujelben, A. Cheikh-Rouhou, and J. C. Joubert, J. Soild State Chem., 156, 2001, p.68.

[19] U. Chand, P. Kumar, and G. D. Verma, Archives of Applied Science Research, 3, 2011,1.

[20] P. Dey, T. K. Nath, Phys. Rev. B, 73, 2006, p.214425.

[21]S. Kundu, and T. K. Nath, AIP Conf. Proc., 1349, 2011, p.453.

[22] R. D. Sánchez, J. Rivas, D. Caeiro, M. Östlund, M. Servin, C.Vázquez, M. A. López-Quintela, M. T. Causa, and S. B. Oseroff, Mater. Sci. Forum, 831, 1997, p.235.

[23] N. Rama, V. Sankaranarayanan, M. S. Ramachandra Rao, J. Appl. Phys., 99, 2006, p.08Q315.

[24] W. Boujelben, M. Ellouze, A. Cheikh-Rouhou, J. Pierre, Q. Cai, W. B. Yelon, K. Shimizu, and C. Dubourdieu, Phys. Stat. Sol., 191, 2002, p.243.

[25] T. Sarkar, A K Raychaudhuri, A. K. Bera, and S. M. Yusuf, New. J. Phys., 12, 2010, p.123026.

[26] H.Y. Hwang, S-W Cheong, N. P. Ong, and B. Batlogg, Phys. Rev. Lett., 77, 1996, p.2041.

[27] P. Raychaudhuri, T. K. Nath, A. K. Nigam, and R. Pinto, J. App. Phys., 84, 1998, p.2048.

[28] G. M. B. Castro, J. Alloys Comp., 369, 2004, p.108.

[29] Hongwei Qin et al., J. App. Phys., 91, 2002, p.12.

[30] A. Yelon, D. Menard, M. Britel, and P. Ciureanu, Appl. Phys. Lett., 69, 1996, p.20.

[31] S. Mollah, Z.A. Khan, D.K. Shukla, M. Arshad, Ravi Kumar, A. Das, J.Phys. Chem.Solids, 69, 2008, p.1023.

[32] S. Kundu and T. K. Nath, J. Phys.: Condens. Matter, 22, 2010, p.506002.

[33] N. F. Mott and E. A. Davies, Electronic Processes in Noncrystalline Solids, 2nd ed. ~Oxford University of Process, New York, 1979; H. Boettger and V. Bryksin, Hopping Conduction in solids, Akademic -Verlag, Berlin, 1951.

[34] M.Viret, L. Ranno, and J. M. D. Coey, Phys. Rev. B, 55, 1996, p.8067.

[35] A. Banerjee, S. Pal, E. Rozenberg, and B. K. Chaudhuri, J. Phys.: Condens. Matter, 13 2001, p.9489.

[36] Proloy T. Das, A. K. Nigam, A. Taraphder, and T. K. Nath (unpublished).

[37] D. Kumar, J. Sankar, J. Narayan, Rajiv K. Singh, and A. K. Majumdar Phys. Rev. B, 65, 2002, p.094407.

[38] Y. Gao, G. Cao, J. Zhang, and H. U. Habermeier, Phys. Rev. B, 85, 2012, p.195128.

Author' biography with Photo

Proloy T. Das is a senior research scholar of the Dept. of Physics, Indian Institute of Technology, Kharagpur, India. He is working with polymers and manganites nanoparticles and thin films. He studies on Microstructual-, Spectroscopic-, Electronic- and Magnetic properties of nanocomposite/ thin films of different morphologies.

Dr. T. K. Nath is a Professor in the Dept. of Physics, Indian Institute of Technology, Kharagpur. He obtained his M.Sc. degree from Indian Institute of Technology Kharagpur in the year 1990 and Ph.D. degree from Indian Institute of Technology Kanpur in the year 1996. He was a postdoctoral fellow in Duke University, USA, North Carolina State University, USA and in Tata Institute of Fundamental Research, India. His research interests include Strongly correlated system, Nanostructured magnetic materials, Magnetic thin films and multilayers, Dilute magnetic semiconductors, Superconductivity, Spintronics, Multiferroics, CMR and GMR materials, Magnetic Metallic Glasses, Highly Spin Polarized Magnetic oxides and Magnetic Huesler alloys for Magnetoelectronics, Magnetocaloric materials etc.. He has more than 100 papers published in various international refereed journals. He is a recipient of prestigious award, "MRSI Medal - 2012" from the Material Research Society of India for his outstanding contribution in Magnetic Materials Research. He has also received the "Royal Society Grant Award - 2008" for the high quality International Researchers from the Royal Society, London. He is an editor of various journals, namely. (a) Journal of Spintronics and Magnetic Nanomaterials (American Scientific Publishers, USA) (b) Data set papers in Nanotechnology (Hindwai publishers, USA).